energies

Article

Correction Method for Logging Curves in Clay-Rich Tight Glutenite Reservoir: Upper Wuerhe Formation in Mahu Oilfield, China

Linsheng Wang [1], Qian Xiong [1], Qingping Jiang [1], Zhifeng Wang [2,*], Zigang Qiu [1], Kai Liu [1], Chuixian Kong [1], Canhua Liu [1] and Xiaoli Zhang [1]

[1] Research Institute of Exploration and Development, PetroChina Xinjiang Oilfield Company, Karamay 834000, China
[2] Seiser Energy Technology (Beijing) Co., Ltd., Beijing 100102, China
* Correspondence: zhifeng.wang@seiser.com.cn

Abstract: Mahu Oilfield is the largest tight glutenite oilfield in the world, and the upper Wuerhe formation is an important succeeding exploration horizon. However, the upper Wuerhe formation in the Mahu 1 zone has a high clay content, which can lead to serious wellbore collapse. Meanwhile, the horizontal well logging is not corrected. These factors lead to the inconsistency between the logging interpretation results and the oil test results. The interpretation precision of the clay content, water saturation, and porosity, which are crucial to reservoir evaluation, is very low. In this paper, a workflow of logging curve correction using multiple methods is proposed. The multiple linear fitting is used to correct boreholes, and then histogram frequency distribution matching is used to standardize multi-well logging curves. Finally, the optimization method is used to build a volume model based on skeleton analysis, and the results are calibrated with core analysis results. Horizontal well density logs are corrected using adjacent vertical well logs. The interpretation results of clay content, water saturation, and porosity with high precision are obtained. The reservoir interpretation is more in line with the oil test results than the original interpretation. The clay content distribution is more reasonable.

Keywords: glutenite reservoir; correction for logging curve; borehole enlargement; clay content; horizontal well

Citation: Wang, L.; Xiong, Q.; Jiang, Q.; Wang, Z.; Qiu, Z.; Liu, K.; Kong, C.; Liu, C.; Zhang, X. Correction Method for Logging Curves in Clay-Rich Tight Glutenite Reservoir: Upper Wuerhe Formation in Mahu Oilfield, China. *Energies* **2022**, *15*, 7119. https://doi.org/10.3390/en15197119

Academic Editors: Shiqing Cheng, Wenyang Shi, Yang Wang and Reza Rezaee

Received: 23 July 2022
Accepted: 22 September 2022
Published: 28 September 2022

1. Introduction

With the depletion of conventional oil and gas resources, unconventional oil and gas resources have become an important strategic succeeding direction. Tight oil resources are abundant, but their development technology is not mature and is still under exploration. Mahu Sag in Junggar Basin, China, is rich in tight oil resources, and it is currently the largest known glutenite oil field in the world [1]. The upper Wuerhe formation in the Mahu 1 zone is an important succeeding exploration horizon for the Mahu tight reservoir. There are a lot of studies on the reservoir accumulation conditions and the main controlling factors, reservoir accumulation mode, reservoir characteristics and controlling factors [2–5], development methods, and development performance of glutenite reservoirs [6–9]. The characteristics of high-quality glutenite reservoirs and sweet points have been reviewed [10,11], and some understandings on the efficient development of tight glutenite reservoirs have been formed [12]. However, the identification of high-quality glutenite reservoirs and the comprehensive evaluation of productive glutenite reservoirs are some of the difficulties encountered in the development of the upper Wuerhe reservoir. The porosity and water saturation of logging interpretation are important indicators for a comprehensive reservoir evaluation. The upper Wuerhe formation is characterized by a relatively high clay content and a relatively strong water sensitivity. The clay content has a great impact on the reservoir's physical properties [13,14]. The existence of argillaceous material reduces the permeability and porosity of the reservoir. It also makes the pore structure complicated and increases the bound water content. The production practice of the upper Wuerhe formation reservoir shows that better production performance is associated with lower clay content. Therefore, the accurate interpretation of clay content is of great significance for reservoir evaluation. However, the early logging interpretation results are poor, and the interpretation accuracy of porosity, water saturation, and clay content is bad. There are many inconsistencies between the logging interpretation results and the oil test results.

The reason why the logging interpretation accuracy of the upper Wuerhe formation is not high is that the environmental impact has not been well corrected, especially the wellbore collapse in the upper Wuerhe formation, which is serious. The mud invasion and formation anisotropy affect the logging results [15–17]. But in the upper Wuerhe formation, the borehole enlargement caused by borehole collapse is the most important factor [18,19]. Due to the reservoir of the upper Wuerhe formation being tight, some horizontal wells are also used for development. For vertical well logging, the axis of the logging tool is approximately perpendicular to the formation, and the environment can be approximately regarded as symmetrical. For horizontal logging, the axis of the logging tool is approximately parallel to the formation, and the environment is asymmetric. Logging results are affected by rock anisotropy, surrounding rock, instrument eccentricity, and other factors [20–22]. At present, the method of vertical well logging interpretation is used for horizontal well logging interpretation. However, due to the different environments between horizontal wells and vertical wells, the original logging data cannot be directly used for interpretation.

For vertical well logging, different environmental corrections have been developed by various companies for their logging instruments through rock physics forward modeling, including plots and empirical formulas [23–25]. For horizontal well logging, rock physics forward modeling is also often used to analyze the influence of horizontal well logging and establish a theoretical correction plot or correction coefficient formula [26,27]. However, these calibrated plots and empirical formulas are developed for different logging instruments and different simulated environmental conditions and have limited applicability. Because the actual formation is often very complex, it is difficult for the current plots and empirical formulas to completely conform to the actual situation, and often good results cannot be obtained. Figuring out how to do environmental correction is still an important subject when it comes to logging interpretation. There exist relationships between different geophysical properties. Therefore, relationships between different logging curves can be established [28–30]. Environmental factors have different effects on different logging curves. Therefore, a logging curve less affected by a certain environmental factor can be used to correct other logging curves [31–33]. For horizontal wells, it is also possible to establish a relationship with adjacent vertical wells on the same horizon to correct the horizontal well logging curves. This allows logging correction methods for specific reservoirs to be established, considering the geological and sedimentary characteristics and complexity of the reservoir. Of course, whether the result of the environmental correction of logging curves is appropriate needs the reference standard of evaluation. However, there is no reference standard for the environmental correction of many logging curves.

In view of the above issues, to improve the interpretation accuracy of logging curves of Wuerhe formation in the Mahu oilfield, especially the interpretation accuracy of clay content, this study fully considers the advantages of various methods. A method of combining various methods to correct logging curves is established. Using high-quality logging curves for multivariate linear fitting, the borehole enlargement is corrected. The logging curves of multiple wells are normalized to eliminate the errors caused by different logging instruments. To establish the volume model, the forward modeling of the petrophysical model is carried out, and the logging interpretation is optimized against corrected logging curves. Therefore, the logging interpretation of the same reservoir is based on the same skeleton parameters. Through the calibration of core analysis results, the corrected logging interpretation results have reference standards. Thus, the accuracy of the logging interpretation is improved, and the results are consistent with the oil test results.

2. Problems in Current Well Logging Interpretation

The reservoir in this area is tight, the in-situ stress changes greatly, and some boreholes collapse seriously. These lead to the distortion of the interpretation results of the density and acoustic logging. Affected by the borehole collapse, most well density curves have unreasonable responses, and the density value of the enlargement section is significantly reduced. The porosity and water saturation of the logging interpretation are quite different from the results of the core analysis, as shown in Figure 1. Another manifestation of low logging interpretation accuracy is that the clay content distribution of conventional interpretation is poorly matched (Figure 2), which has a great impact on the clay content predicted by the well seismic calibration. It brings serious problems to reservoir parameters and reservoir fine evaluation. As a result, the interpretation of some logging curves is unreasonable. This leads to the mismatching of the logging interpretation results of some wells and the conclusion of their oil tests. For example, the P_3w_1 interval of well XX021 and well XX020 in the original logging interpretation is the oil layer. However, the oil test results show that the P_3w_1 interval of XX020 does not produce oil and is not within the scope of the reservoir. The daily oil production of well XX021 is only 0.08 t/d.

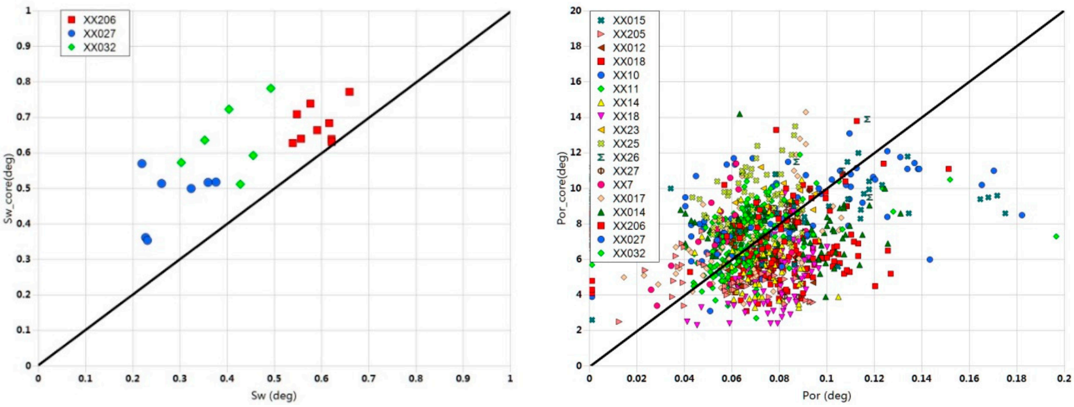

(**a**) (**b**)

Figure 1. Comparisons between original logging interpretation results and core analysis results: (**a**) Water saturation; (**b**) porosity.

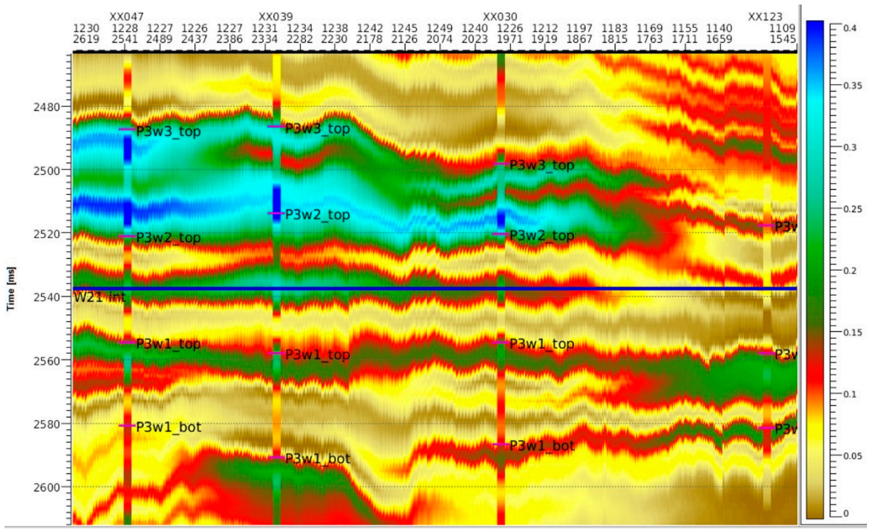

Figure 2. The distribution of the clay content obtained from conventional logging interpretations.

At present, the methods for horizontal well logging interpretation are lacking, and they all use vertical well logging interpretation methods. Because the logging environment of the horizontal well is different from that of the vertical well, when using the vertical well logging interpretation method to interpret, it is necessary to correct the logging curve. The original horizontal well logging interpretation of the upper Wuerhe formation reservoir in the Mahu 1 zone has not been corrected. The production performance of well XX21001 and well XX21012 is very poor. However, nearly 1500 m horizontal sections are interpreted as reservoirs in the original logging interpretation, and the interpreted oil saturation is high. This is not consistent with the actual production performance. Figures 3 and 4 respectively show the histogram comparison of the porosity and water saturation for the logging interpretation of 34 horizontal wells. The distribution characteristics of the original interpretation are quite different from those of the vertical wells, and their distribution range and characteristics are inconsistent.

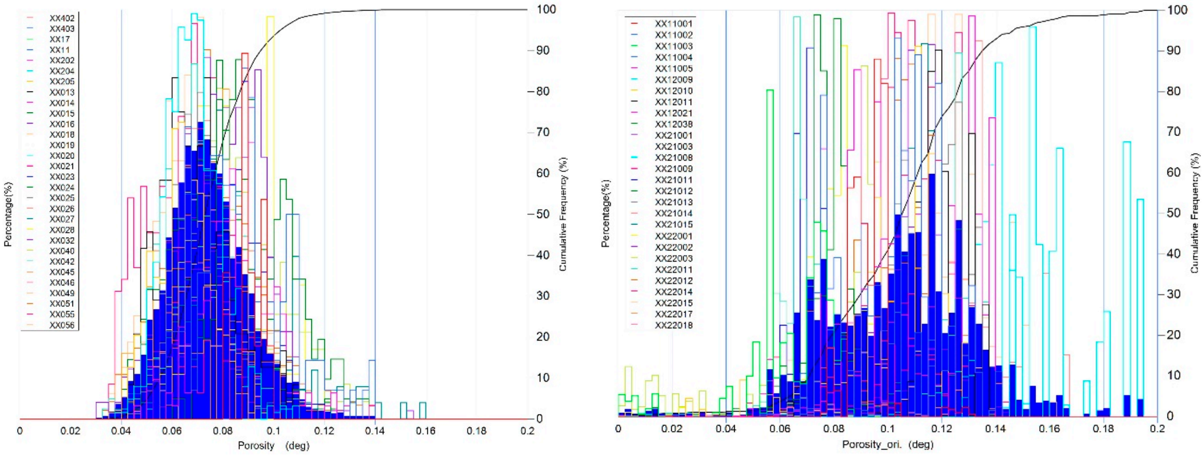

(**a**) (**b**)

Figure 3. Histograms of the porosity for logging interpretation: (**a**) vertical wells; (**b**) horizontal wells (original). The blue-filled histogram is the cumulative distribution of all wells.

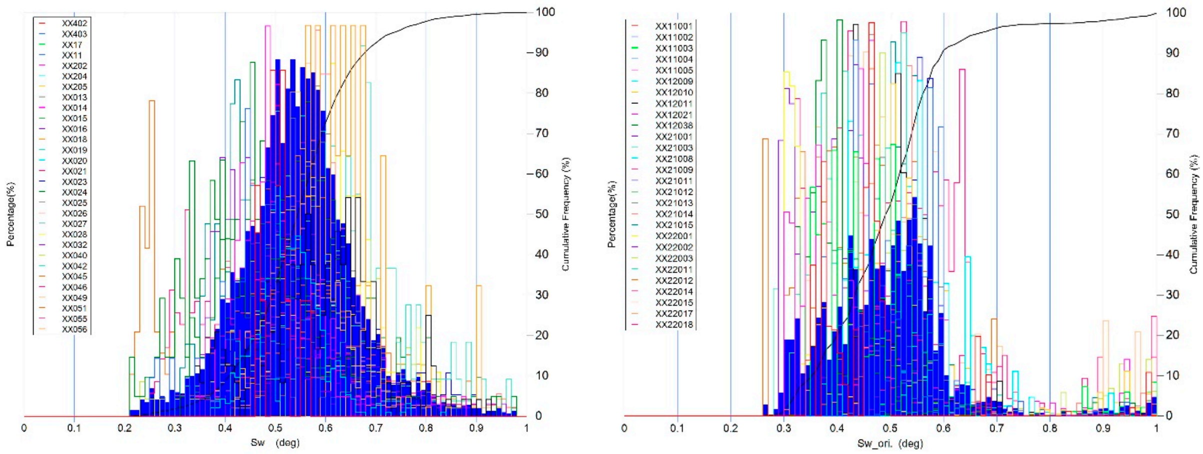

(**a**) (**b**)

Figure 4. Histograms of water saturation for logging interpretation: (**a**) vertical wells; (**b**) horizontal wells (original). The blue-filled histogram is the cumulative distribution of all wells.

3. Correction Method of Well Logging Curves

To get proper logging interpretation results, it is necessary to correct the logging curve. First, the borehole correction is carried out. Then, the multi-well normalization correction is carried out for curves after borehole correction. After that, based on the skeleton analysis, the volume model is established through the optimization method. The results of the core analysis are used to calibrate the logging interpretation results, to reduce the impact of individual error of logging curves. Thus, the volume model consistent with the reservoir and high-precision clay content parameters is obtained, which makes the reservoir results of the logging interpretation consistent with the oil test conclusions.

3.1. Borehole Correction

Different logging instruments have different requirements for borehole conditions. The measuring instrument of the acoustic time difference can compensate for the unevenness and the small collapse of the borehole. The electrode distance of the resistivity instrument is generally larger than the invasion layer, and deep resistivity logging can detect more than 1.4 m. A cylinder volume with a radius of 50–80 cm along the wellbore is measured by the compensated neutron. Therefore, these instruments can measure precise data under small borehole collapse conditions. The density measurement instrument must be attached to the well wall. So, the uneven well wall and small collapse can cause curve distortion. The borehole collapse has a great impact on the density logging curve, while the impact on the logging results of the acoustic time difference, neutrons, and resistivity gradually decreases. For intervals close to each other with similar lithofacies, lithology, and fluid properties, multivariate linear fitting is performed for well-quality logging curves. For non-collapsed intervals, the direct functional response relationship between the benchmark curve and the calculation curves is established using the relationship between the logging response of the density, resistivity, compensated neutrons, and acoustic time difference. Then, the logging response of the density is corrected in poor quality intervals. For the upper Wuerhe formation, the following correction equation is obtained by using the logging curve fitting of non-collapsed intervals with similar lithology and sedimentary:

$$CNL_{\mathrm{jz}} = 0.437207 - 0.254117 \log R_{\mathrm{tn}}, \tag{1}$$

$$DT_{\mathrm{jz}} = 88.3037 - 35.1216 \log R_{\mathrm{tn}} + 55.3088 CNL_{\mathrm{jz}}, \tag{2}$$

$$DEN_{\mathrm{jz}} = 2.47403 + 0.184985 \log R_{\mathrm{tn}} - 0.287586 CNL_{\mathrm{jz}}, \tag{3}$$

where CNL_{jz} is the corrected compensated neutron logging, dec; DT_{jz} is the corrected acoustic time difference logging, μs/m; DEN_{jz} is the corrected compensated density logging, g/cm^3; R_{tn} is the resistivity, Ω·m. Firstly, the resistivity logging, which is least affected by the borehole collapse, is used to correct the compensation neutron logging, which is also less affected. Then, the resistivity and compensated neutron logging are used to correct the third-least affected acoustic time difference logging. Finally, they are used to correct the compensated density logging that is most affected by the borehole collapse. The sequence of the correction considers the extent to which different loggings are affected by the borehole collapse. The well wall collapse in the mudstone section of the upper Wuerhe formation is remarkable, causing varying degrees of impact on different logging curves. The logging response is abnormal, and there exist abnormal points of low density. The data points of the acoustic-neutron, acoustic-density, and neutron-density crossplots are scattered. This is shown in Figure 5. After correction, the abnormal data points are reasonably and effectively repositioned, and the acoustic-neutron, acoustic-density, and neutron-density crossplots have a good relationship.

3.2. Normalization for Logging Curves

In addition to eliminating environmental impacts, logging instruments and operations can cause systematic errors. To improve the comparability of logging results across multiple wells, the logging curve normalization is required to eliminate these errors [34–36]. To normalize logging curves, a layer with basically the same geological deposition is selected as the standard layer. The curved shape and characteristics of the logging response of such layers are basically the same. This standard layer can therefore be calibrated consistently across all wells. Then other layers are corrected according to the correction coefficient of the standard layer, considering the glutenite and mudstone lithologic strata of Wu 2 are stable in the deposition within the scope of the oilfield with large formation thickness. The lithology and logging response characteristics are obvious. Therefore, it is chosen as a standard layer for multiple well consistency processing. Using the method of histogram pattern matching, the consistency check is performed on the curves of the acoustic time difference, neutron, and density logging of multiple wells. The comparison of the histogram probable pattern matching before and after multi-well normalization is shown in Figure 6. The plot pattern matching after normalization is better. Before normalization, the distribution pattern of the multi-well histogram is scattered, and the sample points of different wells are not completely consistent. After normalization, the multi-well histogram patterns are consistent, and the characteristics and standard deviation of the multi-well logging response of the acoustic, neutron, and density for different lithologies are basically consistent.

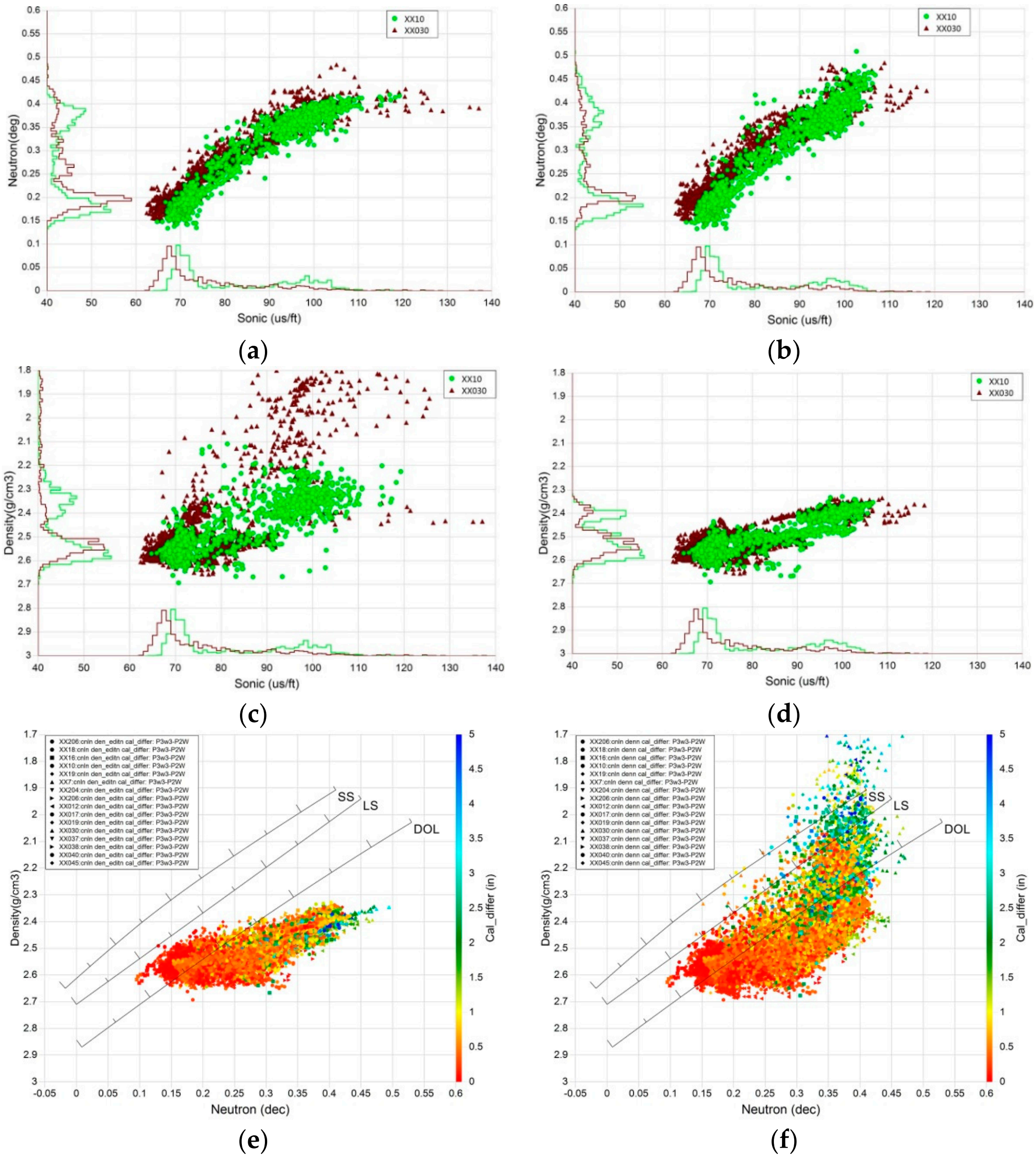

Figure 5. Comparisons of crossplots before and after corrections. (**a**) acoustic-neutron crossplot before corrections. (**b**) acoustic-neutron crossplot after corrections. (**c**) acoustic-density crossplot before corrections. (**d**) acoustic-density crossplot after corrections. (**e**) neutron-density crossplot before corrections. (**f**) neutron-density crossplot after corrections.

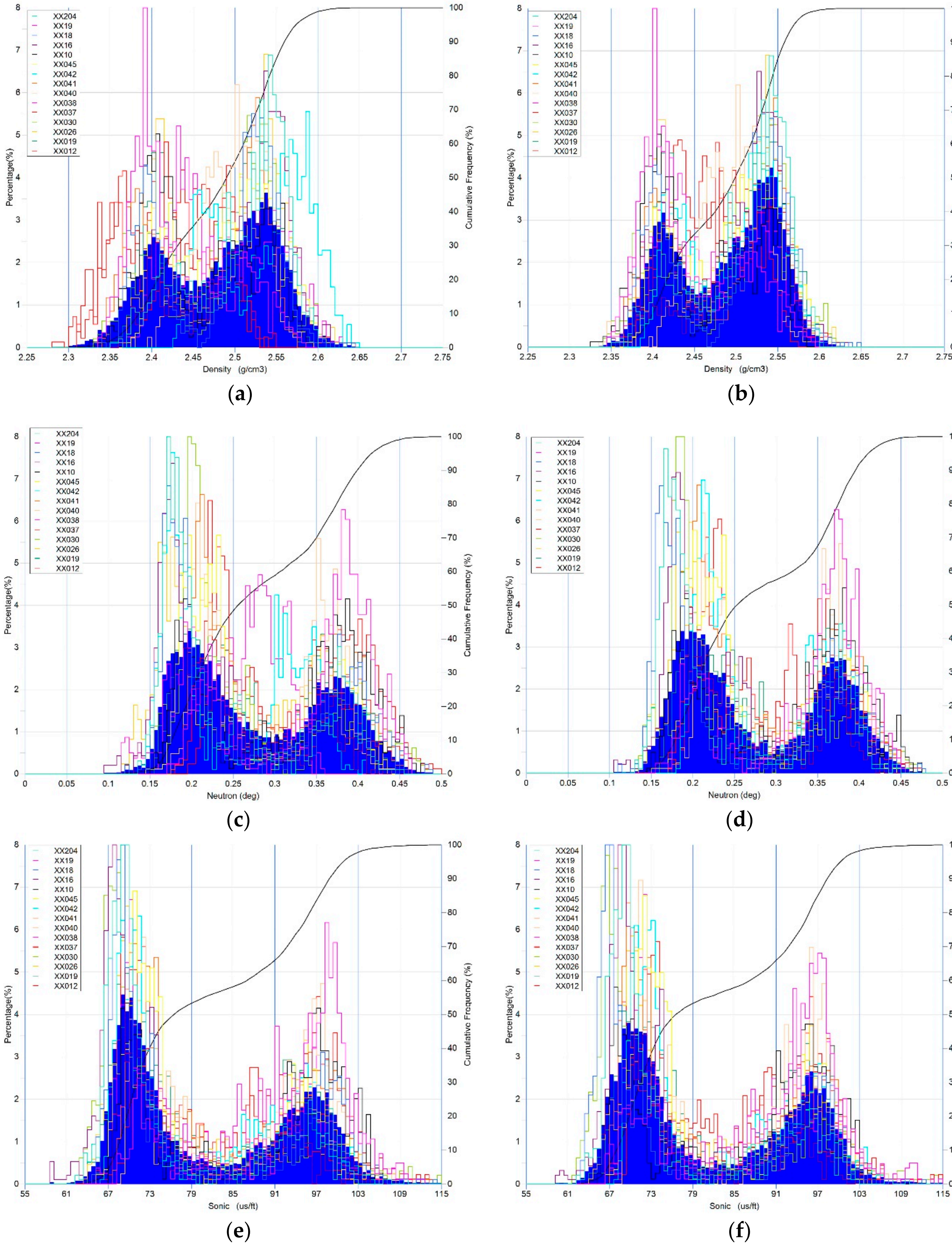

Figure 6. Comparisons of histograms before and after normalization: (**a**) Multi-well density before normalization; (**b**) Multi-well density after normalization; (**c**) Multi-well neutron before normalization; (**d**) Multi-well neutron after normalization; (**e**) Multi-well acoustic before normalization; (**f**) Multi-well acoustic after normalization.

3.3. Mineral Skeleton Parameters

After the borehole correction and normalization processing of multi-well logging curves for well logging data in the upper Wuerhe formation of the Mahu oilfield, the neutron-density crossplot, and acoustic-density crossplot analysis are carried out for the logging data of Wu 2 and Wu 1 intervals to determine the acoustic, neutron, and density logging response parameter values of clay and sandstone skeleton points, as shown in Figures 7 and 8. The vertices A, B, and C of the triangle in the figures are the sandstone skeleton, water point, and clay point, respectively. From the density-acoustic crossplot, the sandstone skeleton point and clay point response characteristics of the density and acoustic logging of the target layer can be determined. From the density-neutron crossplot, the sandstone skeleton point and clay point response characteristics of the density and neutron logging in the target layer can be determined. The neutron, acoustic time difference, and density logging response values of the clay and sandstone skeleton in Wu 1 and Wu 2 intervals obtained from the analysis are listed in Table 1. The logging response values of water points listed in Table 1 are theoretical results. They are used as unified parameters to establish the rock volume model of the upper Wuerhe formation and analyze the reservoir porosity, clay content, and water saturation.

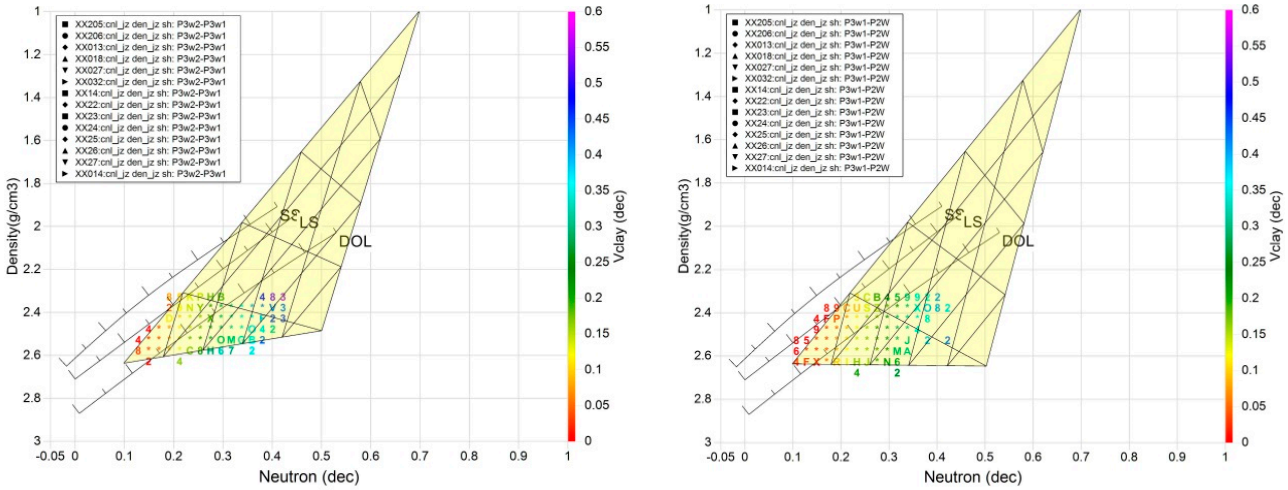

(**a**) (**b**)

Figure 7. The neutron-density crossplot method: (**a**) Wu 2 interval; (**b**) Wu 1 interval.

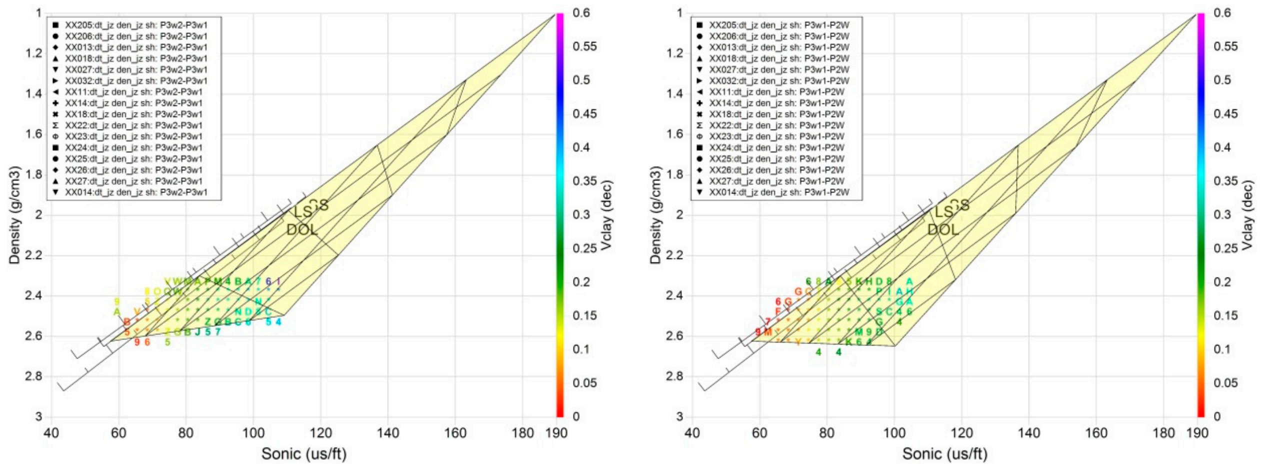

(**a**) (**b**)

Figure 8. The acoustic-density crossplot method: (**a**) Wu 2 interval; (**b**) Wu 1 interval.

Table 1. Parameters for the volume model.

	Wu 2 Interval			Wu 1 Interval		
	V_{Clay}	V_{Qua}	**Water**	V_{Clay}	V_{Qua}	**Water**
Acoustic (us/ft)	107	57	189	100	57	189
Neutron (dec)	0.5	0.1	0.7	0.5	0.1	0.7
Density (g/cm^3)	2.5	2.64	1	2.65	2.64	1

3.4. Volume Model Calculation

When establishing rock volume model, it may be found that the number of logging curves exceeds the unknown number of volume content. Different volume contents may be calculated using different combinations of logging curves. To avoid this situation and make full use of logging data, the volume content is obtained under the same set of logging response parameters, and the optimization method is used to calculate the volume model. Taking the comprehensive error of all logging curves as the optimization objective and the weight coefficient and volume content of different logging curves as the optimization variables, the optimization results are calibrated through the core analysis of clay content and porosity. Therefore, the skeleton parameters of the same layer are the same. The volume content obtained in this way is the average result of all logging curves, which can reduce the influence of the error of individual logging curves on logging interpretation results. The logging response curve of each component's volume content and skeleton parameters are related through the following linear equation:

$$\begin{bmatrix} y_{k1} \\ \vdots \\ y_{kn} \end{bmatrix} = \begin{bmatrix} a_{11} & \cdots & a_{1m} \\ \vdots & & \vdots \\ a_{1n} & \cdots & a_{nm} \end{bmatrix} \begin{bmatrix} x_{k1} \\ \vdots \\ x_{km} \end{bmatrix}, \tag{4}$$

where $x_{k1}, \ldots \ldots, x_{km}$ are the volume contents; $a_{11}, \ldots \ldots, a_{nm}$ are logging response parameters of the skeleton, clay, fluid, etc; $y_{k1}, \ldots \ldots, y_{km}$, etc. are logging response curves; n is the number of logging curves; m is the number of volume component; k is the kth measuring point of the logging curve. The volume content meets the constraints of normalization:

$$\sum_{i=1}^{m} x_{ki} = 1, \tag{5}$$

The optimization objective function is as follows:

$$Y = \sum_{k} \sum_{i=1}^{n} \alpha_i (y_{ki}^c - y_{ki})^2 a = 1, \tag{6}$$

where α_i is the weight coefficient of the ith logging curve; y_{ki}^c is the corrected measured value of the ith logging curve. By minimizing Y, the optimal values of the volume content and weight coefficient are obtained. Table 1 shows the skeleton logging response parameters used for the optimization.

Figure 9 shows the results of the optimized volume model of well XX206. The logging curve obtained from the forward modeling of the volume model is very close to the corrected actual logging curve, and the optimized clay content and porosity are in good agreement with the results of the core analysis.

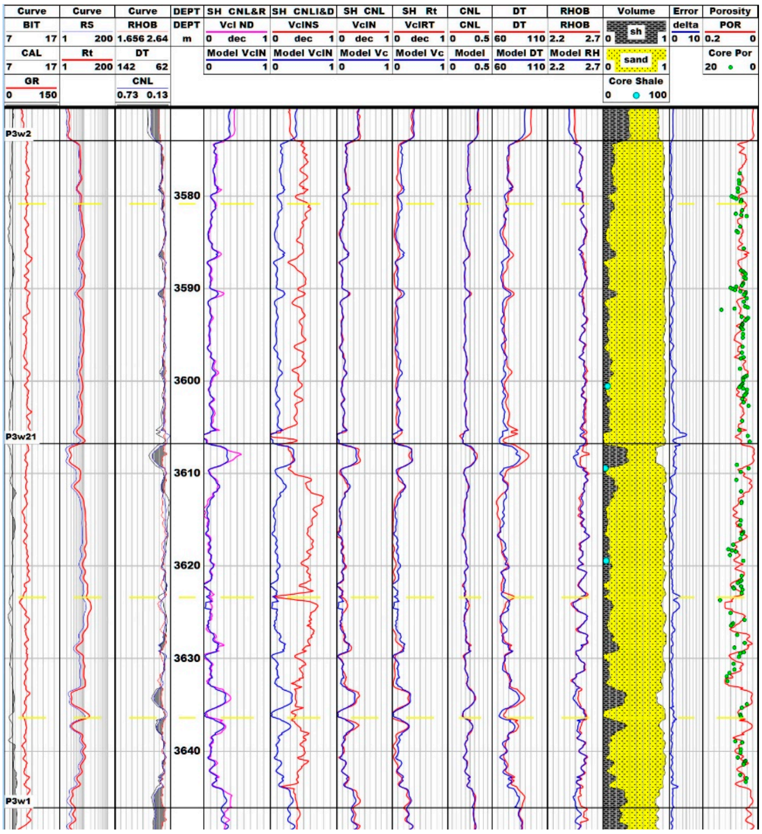

Figure 9. Comparisons between the logging curves (blue) calculated by the optimized volume model and the original curves (red). The purple curve is the clay content calculated by density-neutron crossplot. The green points are the core porosity. The rose curve is the density.

4. Logging Interpretation for Vertical Wells

4.1. Logging Interpretation Results

After the logging data correction, logging interpretation results of the porosity, clay content, and water saturation with high accuracy are obtained. Figure 10 shows the comparisons between the original interpretation of the clay content, porosity, and water saturation and the current interpretation results, as well as the comparisons between the current interpretation results and the core analysis results. The accuracy of the current interpretation results has been greatly improved compared with the original interpretation results. The current logging interpretation results are in good agreement with the core analysis results. Compared with the results of the core analysis, the clay content interpretation results of 16 wells with 72 data points have an interpretation accuracy of 80% and an average absolute error of 1.6%. The porosity interpretation results of 23 wells with 998 data points have an interpretation accuracy of 88% and an average absolute error of 0.4%. The water saturation logging interpretation results of 3 wells with 22 data points have an interpretation accuracy of 92% and an average absolute error of 0.03. The correlation line between logging interpretation results and core analysis results has a 45° slope. This shows that the logging interpretation result is good. The average absolute error is the average of the absolute error between the logging interpretation results and the core analysis results. Figure 11 shows the distribution of the clay content after correction. The distribution of the clay content interpolated between wells after correction is reasonable and the matching is good. Compared with the distribution of clay content after conventional treatment in Figure 2, it can be found that the matching has been greatly improved.

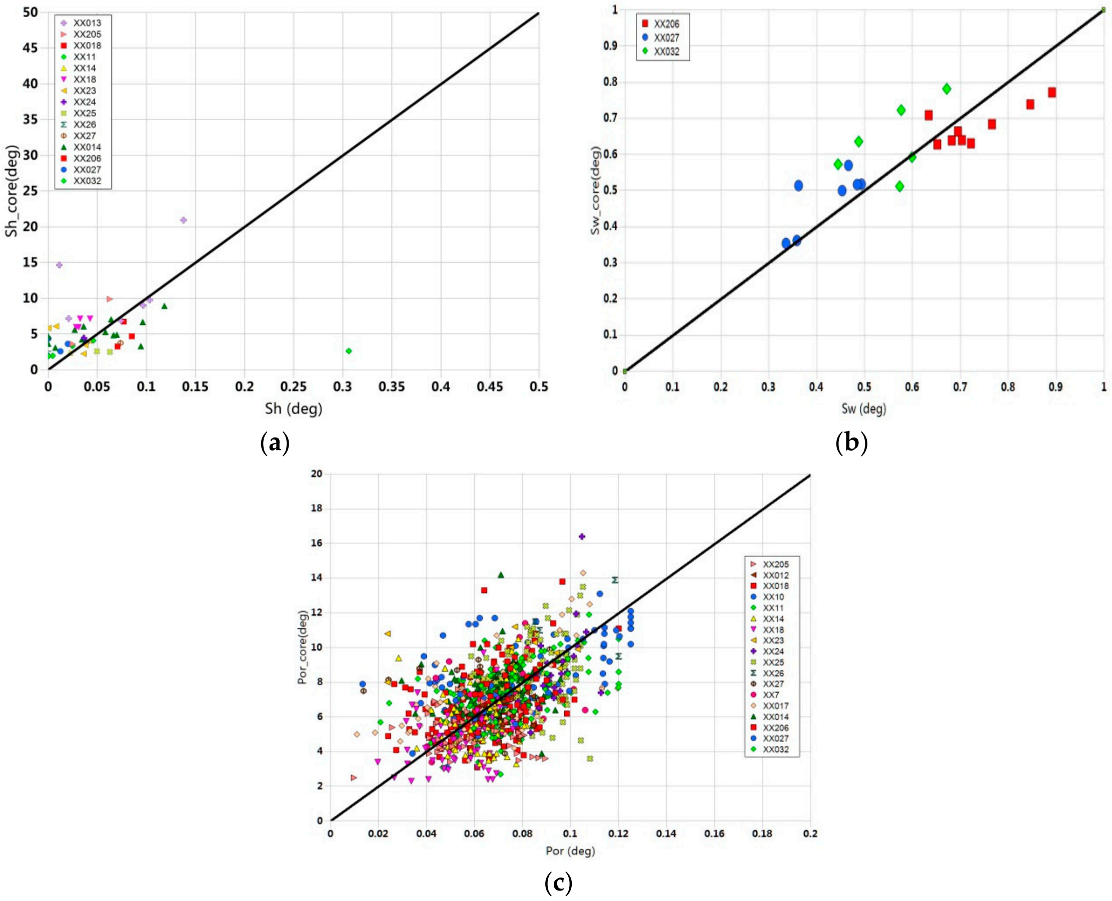

Figure 10. Comparisons between logging interpretation results and core analysis results: (**a**) clay content; (**b**) water saturation; (**c**) porosity.

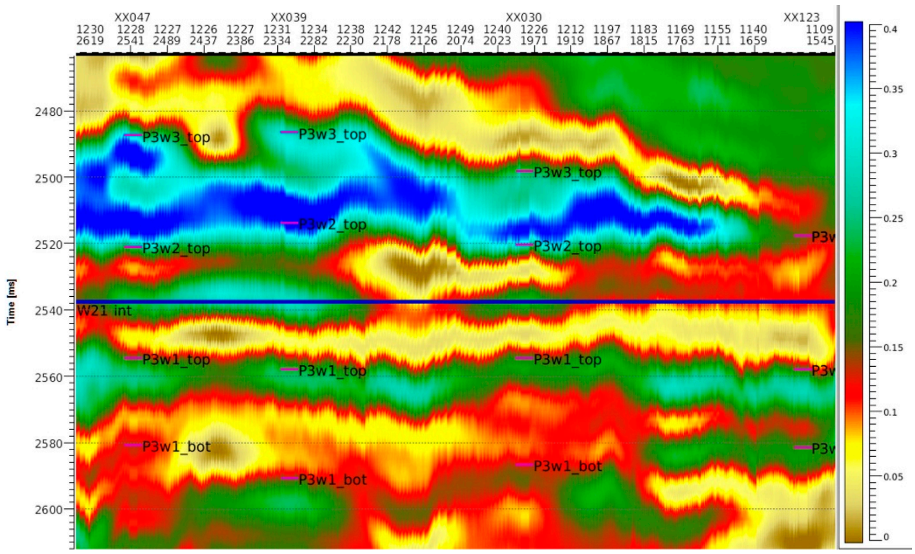

Figure 11. The distribution of clay content after correction.

4.2. Reservoir Interpretation

Using typical rock samples in this area, the resistivity R of 100% saturated brine and resistivity R_t at different water saturation S_w and corresponding porosity ϕ were measured in the laboratory. Fitting F-ϕ and I-S_w curves, the parameters of the Archie equation are obtained as shown in Table 2. By drawing the density porosity-resistivity crossplot of the log interpretation results of the oil test section, the reservoir standard can be drawn. The density porosity-resistivity crossplot of P_3w_2 and P_3w_1 of upper Wuerhe formation in the Mahu 1 zone is shown in Figure 12. From this, the oil layer standard of P_3w_2 of upper Wuerhe formation in Mahu 1 zone is obtained: resistivity $\geq 6.5\ \Omega\cdot$m, porosity $\geq 5.8\%$ and oil saturation $\geq 41\%$; The oil layer standard of P_3w_1 layer: resistivity $\geq 9.5\ \Omega\cdot$m, porosity $\geq 6.0\%$ and oil saturation $\geq 40\%$.

Table 2. Parameters for the Archie equation.

	m	*n*	*a*	*b*	R_w (Ω·m)
Wu 1 interval	1.564	2.029	1.010	1.067	0.090
Wu 2 interval	1.563	1.912	0.843	1.023	0.090

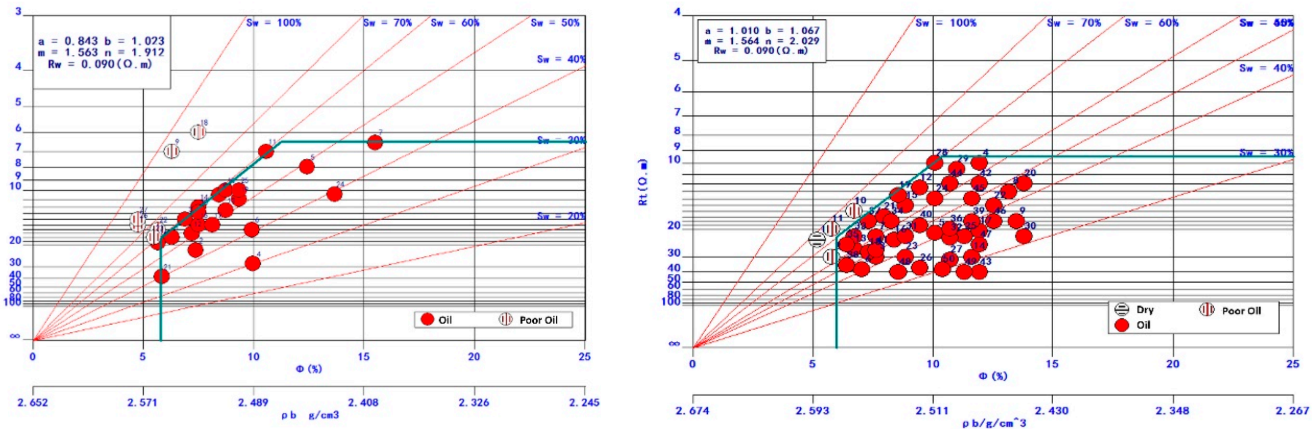

(**a**) (**b**)

Figure 12. The resistivity—density, porosity crossplot: (**a**) P_3w_2 layer; (**b**) P_3w_1 layer.

The thickness of the oil layer interpreted after correction is quite different from that of the originally interpretation for some wells. However, the interpretation results after correction are more consistent with the oil tests and reservoir understanding. The reservoir interpretation results of 7 out of 27 wells interpreted by the original logging curve are inconsistent with the oil test results. After correcting the logging curve, the reservoir interpretation of individual wells is clearer, and the logging interpretation is more consistent with the oil test results. For example, the production test conclusion of well XX046 shows that both P3w1 and P_3w_2 are oil layers. The combined test of the P_3w_2 layer obtained a daily oil production of 10.07 t/d and a cumulative oil production of 154.8 t; the combined test of the P_3w_1 layer obtained a daily oil production of 0.92 t/d and a cumulative oil production of 66.14t/d. According to the current interpretation of the oil saturation, $P_3w_2^1$ is an oil layer with 1 m thickness, $P_3w_2^2$ is an oil layer with 14 m thickness, $P_3w_1^2$ is an oil layer with 5 m thickness, and $P_3w_1^3$ is an oil layer with 8 m thickness. The original logging interpretation interprets these two test intervals as dry layers. Well XX030 has conducted a combined test for the P_3w_2 layer, with a daily oil production of 11.11 t/d and a cumulative oil production of 228.7 t. The combined test of the P_3w_1 layer obtained a daily oil production of 1.4 t/d and a cumulative oil production of 37.5 t/d. The oil test results show that both P_3w_2 and P_3w_1 layers are oil layers. According to the current interpretation of the oil saturation, $P_3w_1^2$ and $P_3w_1^3$ are oil layers with 5 m thickness, and $P_3w_2^1$ and $P_3w_2^2$ are oil layers with 9 m thickness. However, the original logging interpretation results interpreted the P_3w_1 test interval as a dry layer. After the curve correction, these oil testing layers can be correctly interpreted as oil layers. The original logging interpretation results and the current logging interpretation results are shown in Figure 13.

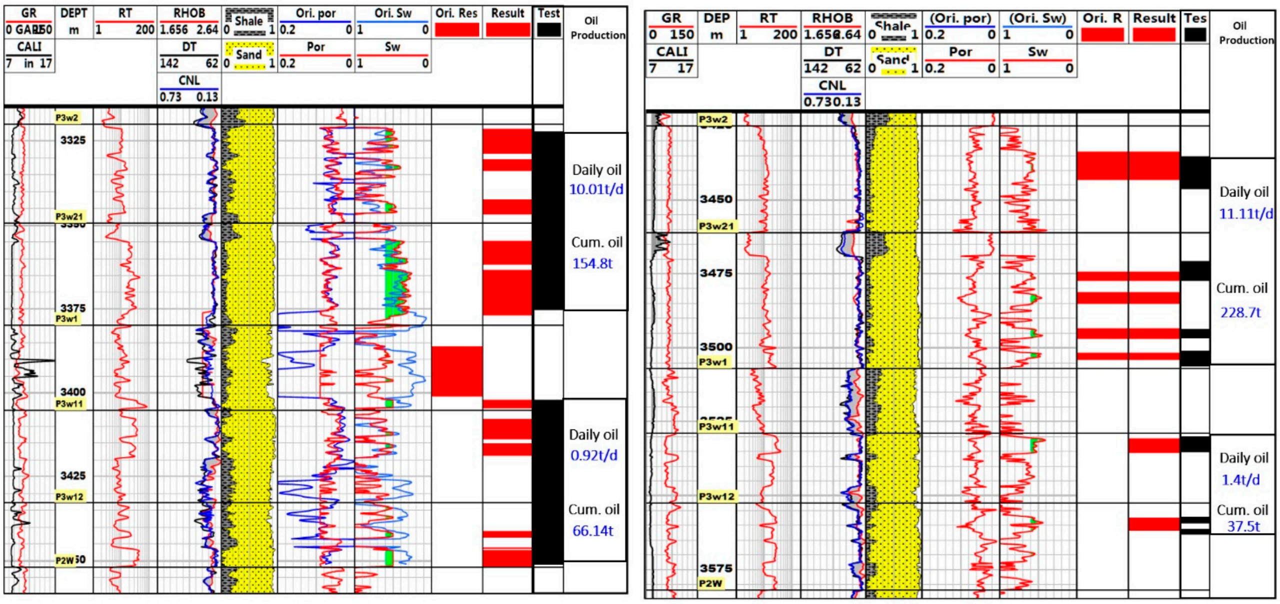

(**a**) (**b**)

Figure 13. The plot of the logging interpretation results: (**a**) Well XX046; (**b**) Well XX030.

5. Logging Interpretation for Horizontal Wells

The horizontal well logging instrument is in an approximate horizontal state, and its logging response must be different from the layered response characteristics of vertical logging. Although logging instrument companies have set up eccentric correction equipment, systematic errors still exist for tight sandstone reservoirs. Therefore, these errors need to be considered. It can be found that there is a great contradiction between the porosity and permeability calculated by the density or acoustic logging and the actual production performance. It is mainly caused by the anisotropy of the formation and the eccentricity of the logging tool. The sound propagates along the fastest path, and there is a big difference between horizontal and vertical states. The density is measured by the response of rocks in a cylinder, which reduces the influence of the horizontal well instrument eccentricity and formation anisotropy. Since the thickness of the target layer in this area is more than 6m, the influence of surrounding rock on horizontal well logging can be ignored. Because horizontal well logging is timely logging, its borehole is basically intact. In the method proposed here, only the density logging is corrected, and the density logging curve is used for the porosity calculation.

The density logging curve is the core logging curve for the porosity interpretation. The reservoir deposition in this area is stable, and the overall change of the sand body near the horizontal trajectory is small. According to the distribution characteristics of the sand body density logging curve of the vertical well (the target sand body drilled by the horizontal well), the sand body density logging curve of the horizontal well is adjusted. Then, the density distribution profile of the horizontal well is consistent with that of the vertical wells. After the density response of horizontal wells is corrected to the response characteristics of vertical wells, the logging interpretation method of vertical wells can be used to process and interpret the logging curve of horizontal wells, including the clay content calculation, volume model interpretation, porosity interpretation, oil saturation interpretation, and reservoir interpretation.

The logging interpretation results of well XX21012 and well XX21001 are shown in Figures 14 and 15, respectively. The porosity of well XX21001 is significantly smaller than the original calculation, and the oil saturation and the oil layer thickness are significantly reduced. The production performance of this well is extremely poor, with an average daily output of 3.3 m^3 and a cumulative output of 2013 t; the porosity of well

XX21012 is similar between two calculations, and the thickness of the oil layer is slightly reduced. But the oil saturation is significantly reduced. With an average daily output of 14.3 m^3 and a cumulative output of 2746 t, the production of this well is poor. Compared with the original interpretation results, this interpretation is in good agreement with the production performance.

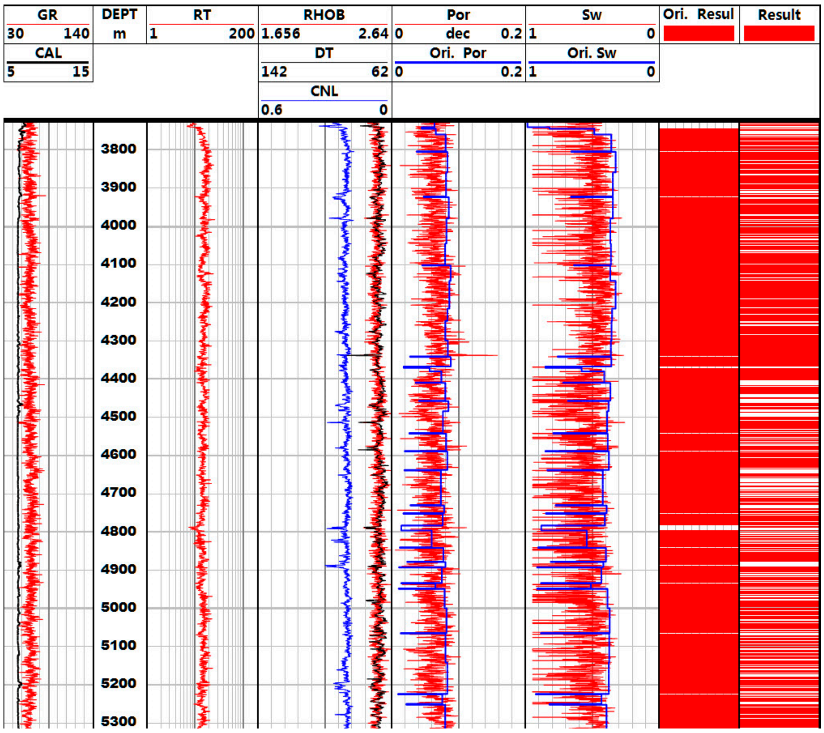

Figure 14. The logging interpretation result for Well XX21012.

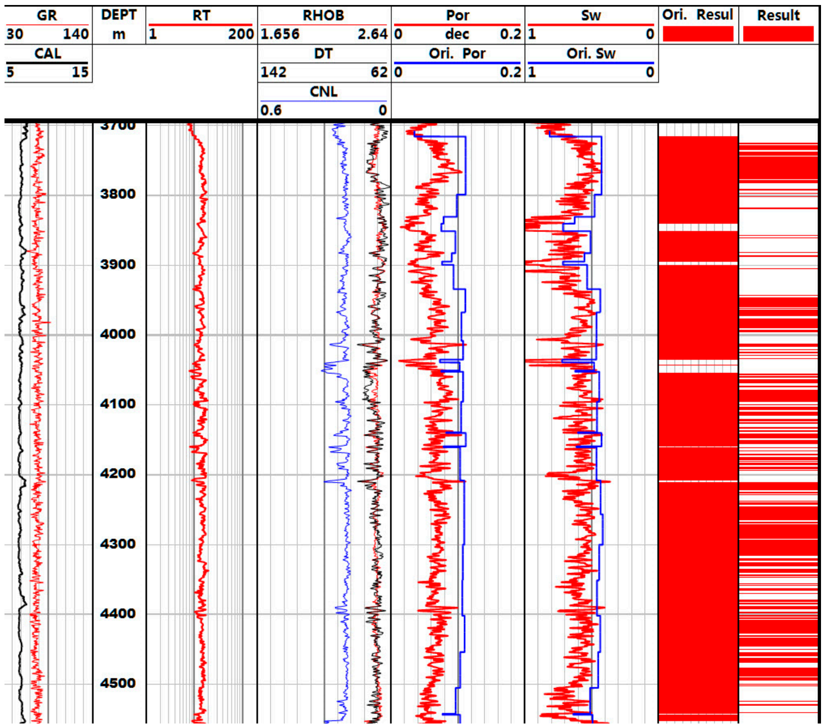

Figure 15. The logging interpretation result for Well XX21001.

Figure 16 shows the histogram of the porosity and water saturation for the logging interpretation of 34 horizontal wells. Compared with Figures 3 and 4, it can be found that the distribution range and characteristics of the interpreted reservoir porosity and water saturation are like that of adjacent vertical wells in the same layer, but the value is slightly larger, which is generally reasonable.

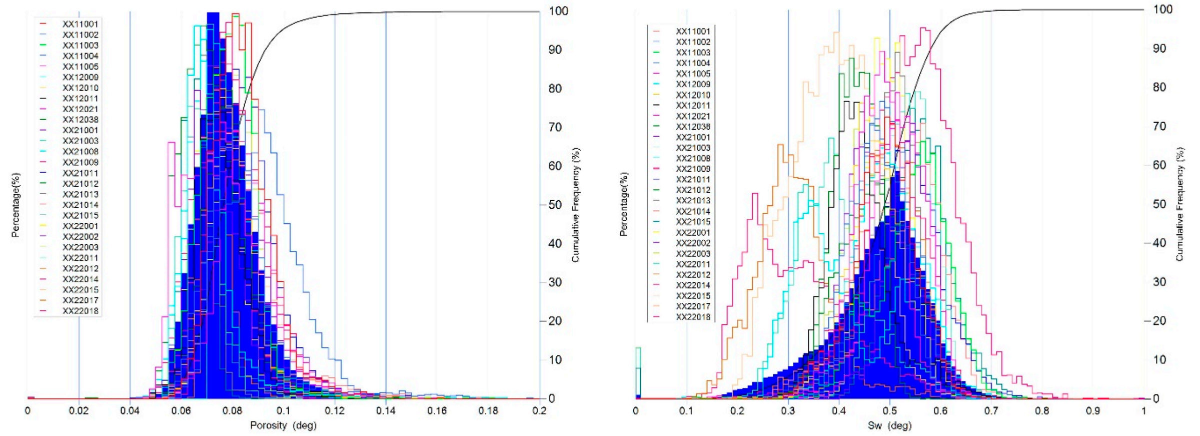

(**a**) (**b**)

Figure 16. Histograms of porosity and water saturation distributions for logging interpretation of horizontal wells: (**a**) porosity; (**b**) water saturation. The blue filled histogram is the cumulative distribution of all wells.

6. Conclusions

The upper Wuerhe formation in the Mahu 1 zone is tight with a high clay content, and horizontal wells are adopted by some wells. There exist serious borehole collapses in vertical wells, which leads to the distortion of density logging curves. The logging curve of the horizontal wells is not reasonably corrected. The interpretation accuracy of the porosity, water saturation, and clay content, which are crucial to the comprehensive evaluation of reservoirs, is low. The logging interpretation results are inconsistent with the oil test results. To improve logging interpretation accuracy, the borehole correction is carried out through multivariate linear fitting. Then, the multi-well logging curve normalization is carried out by using the histogram frequency distribution matching method. After these corrections, the volume model is established by using the same set of logging response parameters in the same layer. The calibration is carried out using core analysis results. The density logging of horizontal wells is corrected using the logging curve of adjacent vertical wells. The porosity and clay content of the logging interpretation are in good agreement with the results of the core analysis. The reservoir interpretation results are more in line with the oil test results. The matching of clay content distribution is greatly improved. The porosity and water saturation distribution characteristics of horizontal wells and adjacent vertical wells tend to be consistent. Thus, a workflow for logging curve correction using multiple methods is established.

Author Contributions: Conceptualization, L.W. and Z.W.; methodology, Q.X. and Q.J.; validation, Q.X., Z.Q. and K.L.; formal analysis, X.Z., C.L. and C.K.; investigation, K.L.; writing—original draft preparation, Z.W., Q.J. and K.L.; writing—review and editing, L.W., Z.W., C.K. and Z.Q.; funding acquisition, L.W. All authors have read and agreed to the published version of the manuscript.

Funding: This research was funded by the Major Science and Technology Project of PetroChina, grant number 2017E-0415 and 2017E-0405.

Institutional Review Board Statement: Not applicable.

Informed Consent Statement: Not applicable.

Data Availability Statement: Not applicable.

Conflicts of Interest: The authors declare no conflict of interest.

References

1. Cao, J.; Zhang, Y.; Hu, W.; Yao, S.; Wang, X.; Zhang, Y.; Tang, Y. The Permian hybrid petroleum system in the northwestern margin of the Junggar basin, northwest China. *Mar. Petrol. Geol.* **2005**, *22*, 331–349. [CrossRef]
2. Tao, K.; Cao, J.; Wang, Y.; Ma, W.; Xiang, B.; Ren, J.; Zhou, N. Geochemistry and origin of natural gas in the petroliferous Mahu Sag, northwestern Junggar basin, NW China: Carboniferous marine and Permian lacustrine gas systems. *Org. Geochem.* **2016**, *100*, 62–79. [CrossRef]
3. Wang, J.; Ge, H.; Liu, J.; Shen, Y.; Zhang, Z.; Luo, S.; Liu, D. Effects of gravel size and content on the mechanical properties of conglomerate. *Rock Mech. Rock Eng.* **2022**, *55*, 2493–2502. [CrossRef]
4. Yuan, G.; Cao, Y.; Qiu, L.; Chen, Z. Genetic mechanism of high-quality reservoirs in Permian tight fan delta conglomerates at the northwestern margin of the Junggar basin, northwestern China. *AAPG Bull.* **2017**, *101*, 1995–2019. [CrossRef]
5. Kang, X.; Hu, W.; Cao, J.; Wu, H.; Xiang, B.; Wang, J. Controls on reservoir quality in fan-deltaic conglomerates: Insight from the lower Triassic Baikouquan formation, Junggar basin, China. *Mar. Petrol. Geol.* **2019**, *103*, 55–75. [CrossRef]
6. Zhu, N.; Cao, Y.; Xi, K.; Wu, S.; Zhu, R.; Yan, M.; Ning, S. Multisourced CO_2 injection in fan delta conglomerates and its influence on reservoir quality: Evidence from carbonate cements of the Baikouquan formation of Mahu Sag, Junggar basin, Northwestern China. *J. Earth Sci.* **2021**, *32*, 901–918. [CrossRef]
7. Gao, H.; Pu, W. Experimental study on supercritical co2 huff and puff in tight conglomerate reservoirs. *ACS Omega* **2021**, *6*, 24545–24552. [CrossRef]
8. Yi, Y.; Wang, L.; Li, J.; Chen, S.; Tian, H.; Tian, G. Optimization of re-fracturing method and fracture parameters for horizontal well in Mahu conglomerate oil reservoir. *Front. Energy Res.* **2022**, *10*, 856524. [CrossRef]
9. Deng, S.; Lü, W.; Liu, Q.; Leng, Z.; Li, T.; Liu, H.; Gu, H.; Xu, C.; Zhang, X.; Lu, X. Research on oil displacement mechanism in conglomerate using CT scanning method. *Petrol. Explor. Dev.* **2014**, *41*, 365–370. [CrossRef]
10. Meng, X.; Wu, S.; Yuan, X.; Xie, Z. Conglomerate reservoir pore evolution characteristics and favorable area prediction: A case study of the lower Triassic Baikouquan formation in the northwest margin of the Junggar basin, China. *J. Earth Sci.* **2021**, *32*, 998–1010.
11. Yu, Z.; Wang, Z.; Jiang, Q.; Wang, J.; Zheng, J.; Zhang, T. Analysis of factors of productivity of tight conglomerate reservoirs based on random forest algorithm. *ACS Omega* **2022**, *7*, 20390–20404. [CrossRef] [PubMed]
12. Li, G.; Qin, J.; Xian, C.; Fan, X.; Zhang, J.; Ding, Y. Theoretical understandings, key technologies and practices of tight conglomerate oilfield efficient development: A case study of the Mahu oilfield, Junggar basin, NW China. *Petrol. Explor. Dev.* **2020**, *47*, 1275–1290. [CrossRef]
13. Yabe, S.; Fukuchi, R.; Hamada, Y.; Kimura, G. A new method for the empirical conversion of logging data to clay mineral fraction in the Nankai accretionary prism. *Earth Planets Space* **2020**, *72*, 166. [CrossRef]
14. Díaz-Curiel, J.; Miguel, M.J.; Biosca, B.; Arévalo-Lomas, L. Gamma ray log to estimate clay content in the layers of water boreholes. *J. Appl. Geophys.* **2021**, *195*, 104481. [CrossRef]
15. Liu, Z.; Tang, X.; Shi, M.; Yang, J. Environmental impact correction for resistivity logging in CBM horizontal well. *IOP Conf. Ser. Earth Environ. Sci.* **2020**, *546*, 022006. [CrossRef]
16. Zhong, X.; Niu, H.; An, Q.; Liu, T. A Two-step Method for Log Correction and Its Application Effect Analysis. *Offshore Oil* **2020**, *40*, 60–66.
17. Kang, Z.; Ke, S.; Jiang, M.; Yin, C.; Li, A.; Li, J. Environmental corrections of a dual-induction logging while drilling tool in vertical wells. *J. Appl. Geophys.* **2018**, *151*, 309–317. [CrossRef]
18. Liu, Z.; Zhao, J. Correcting hole enlargement impacts on density logs for coalbed methane reservoirs. *Open Petrol. Eng. J.* **2015**, *8*, 72–77. [CrossRef]
19. de Macedo, I.A.S.; de Figueiredo, J.J.S.; de Sousa, M.C. Density log correction for borehole effects and its impact on well-to-seismic tie: Application on a North Sea data set. *Interpretation* **2020**, *8*, 43–53. [CrossRef]
20. Brady, J.L.; Watson, B.A.; Warner, D.W.; North, R.J.; Sommer, D.M.; Colson, J.L.; Kleinberg, R.L.; Wolcott, D.S.; Sezginer, A. Improved production log interpretation in horizontal wells using a combination of pulsed neutron logs, quantitative temperature log analysis, time lapse LWD resistivity logs and borehole gravity. In Proceedings of the 1998 SPE Western Regional Meeting, Bakersfield, CA, USA, 10–13 May 1998.
21. Wang, X.; Chen, H.; Lu, H. Research status of horizontal well logging interpretation in china. *IOSR J. Eng.* **2014**, *4*, 49–52. [CrossRef]
22. Zhou, J. Uncertainty in geosteering and interpretation of horizontal wells -The necessity for constraints and geometric models. *Lead. Edge* **2015**, *34*, 492–499. [CrossRef]
23. de Macedo, I.A.S.; de Souza, M.C.; de Figueiredo, J.J.S. The impact of density log correction on the well-to-seismic-tie: Application on real seismic/well log data. In Proceedings of the 8th Brazilian Symposium on Geophysics, Salinópolis, Brazil, 18–20 September 2018.
24. Lehmann, K. Environmental corrections to gamma-ray log data: Strategies for geophysical logging with geological and technical drilling. *J. Appl. Geophys.* **2010**, *70*, 17–26. [CrossRef]

25. Galford, I.E.; Flaum, C.; Gilchrist, W.A., Jr.; Soran, P.D.; Gardner, J.S. improved environmental corrections for compensated neutron logs. *SPE Form. Eval.* **1988**, *3*, 371–376. [CrossRef]
26. Ghosh, S. A review of basic well log interpretation techniques in highly deviated wells. *J. Pet. Explor. Prod. Technol.* **2022**, *12*, 1889–1906. [CrossRef]
27. Calvert, S.E.E. Log Interpretation in Horizontal Wells. Ph.D. Thesis, University of Leicester, Leicester, UK, 2002.
28. Calderon, J.; Castagna, J. Porosity and lithologic estimation using rock physics and multi-attribute transforms in Balcon field, Colombia. *Lead. Edge* **2007**, *26*, 142–150. [CrossRef]
29. Pramanik, A.; Singh, V.; Vig, R.; Srivastava, A.K.; Tiwary, D.N. Estimation of effective porosity using geostatistics and multi-attribute transforms: A case study. *Geophysics* **2004**, *69*, 352–372. [CrossRef]
30. Russell, B.; Hampson, D.; Todorov, T.; Lines, L. Combining geostatistics & multi-attribute transforms: A channel sand case study. *J. Petrol. Geol.* **2002**, *25*, 97–117.
31. Díaz-Curiel, J.; Miguel, M.J.; Biosca, B.; Medina, R. Environmental correction of gamma ray logs by geometrical/empirical factors. *J. Petrol. Sci. Eng.* **2019**, *173*, 462–468. [CrossRef]
32. Chakraborty, S.; Yadav, A.; Chatterjee, R. Comprehensive rock physics, petrophysics workflow to correct sonic logs for improved seismic QI: Study using wells of Krishna Godavari basin. *J. Appl. Geophys* **2021**, *192*, 104394. [CrossRef]
33. Lapkovsky, V.V.; Istomin, A.V.; Kontorovich, V.A.; Berdov, V.A. Correlation of well logs as a multidimensional optimization problem. *Russ. Geol. Geophys.* **2015**, *56*, 487–492. [CrossRef]
34. Faqihi, M.M.; Crossouard, P.A. Calibration of old well log data using a multiwell environment. In Proceedings of the SPE Middle East Oil Technical Conference & Exhibition, Manama, Bahrain, 3–6 April 1993; Available online: https://admin.onepetro.org/SPEMEOS/proceedings-abstract/93MEOS/All-93MEOS/SPE-25673-MS/55679 (accessed on 22 July 2022).
35. Shier, D.E. Well log normalization: Methods and guidelines. *Petrophysics* **2004**, *45*, 268–280.
36. Quaratero, E.M.; Bechtel, D.; Leier, A.L.; Bentley, L.R. Gamma-ray normalization of shallow well-log data with applications to the Paleocene Paskapoo formation, Alberta. *Can. J. Earth Sci.* **2014**, *51*, 327–340. [CrossRef]